

# Numerical Simulation of Field Vane Shear Test Using Finite Element Method



Anand M. Hulagabali, Pankaj Bariker, C. H. Solanki, and G. R. Dodagoudar

## 1 Introduction

The vane shear test is one of the most widely used methods for the determination of undrained strength due to its low cost and ease of use. However, despite its common usage, the interpretation of the vane test has been quite often a controversial issue. The following are the main shortcomings of the equipment and the usual sources of error in the estimation of the undrained strength: vane size effects, blade thickness effects, soil anisotropy effects, strain rate effects, and progressive failure. The conventional interpretation of field vane shear results did not take into account those effects. So far, over more than a half-century of research and application in geotechnical practice, field vane shear testing has been shown to reflect several heavily criticized with the reliability of the undrained shear strength measured with the vane [11]. These criticisms have centered on conventional interpretation of the measurement of the undrained strength due to merely considering the peak torque and diameter of the vane to calculate  $S_u$ .

Thus, this paper aims to study some of these effects through a finite element analysis (FEA) with appropriate soil models in PLAXIS 3D.

The field vane shear test consists of four rectangular blades fixed at  $90^\circ$  angles to each other. The analysis is carried out by forcing the vane into the ground to the

---

A. M. Hulagabali (✉)  
National Institute of Engineering (NIE), Mysuru 570008, India  
e-mail: [anandmh@nie.ac.in](mailto:anandmh@nie.ac.in)

P. Bariker  
National Institute of Technology Karnataka, Surathkal, India

C. H. Solanki  
Civil Engineering Department, SVNIT, Surat 395007, India

G. R. Dodagoudar  
Civil Engineering Department, IIT Madras, Chennai 600036, India

desired depth and manually turning the vane rod from the vane handle located at the upper end until the soil achieves its failure mode to measure the peak torque applied [8]. The peak torque applied to the soil was converted into undrained shear strength,  $S_u$ , using the conventional interpretation.

The study addresses the described general objective and tries to investigate the factors influencing the result of filed vane shear test using finite element. The finite element code PLAXIS 3D is used for the numerical simulation with different soil models, the input parameters of each material model derived from the literature work. The result of the numerical analysis was compared with the conventional analysis method.

## 2 Literature Review

Several researchers have discussed the nature of the disruption caused during vane insertion and measured potential soil disturbance. According to the studies of Wilson et al. [17], strength attained using field vane shear test can be particularly affected by confined soil destruction because of the loss of inter-particle bonds within the soils.

According to Morin [10], the disturbance due to typical blades may result in strength degradation between 10 and 25% of the strength. Insertion disturbance can inconsistently affect both the peak strength and residual strength [3], controlling the accuracy by which soil sensitivity is measured with the vane test.

Cerato and Lutenegeger [3] investigated that disturbance induced by inserting a vane should be linked to the geometry of the field vane shear for the same soil. It is reasonable that the more soil that must be displaced to permit the vane to be inserted, the more the amount of disturbed soil. The level of disturbance caused by the field vane shear is measured as shown in Fig. 1. And also at every depth, the undrained shear strength is shown to decrease with increasing blade thickness.

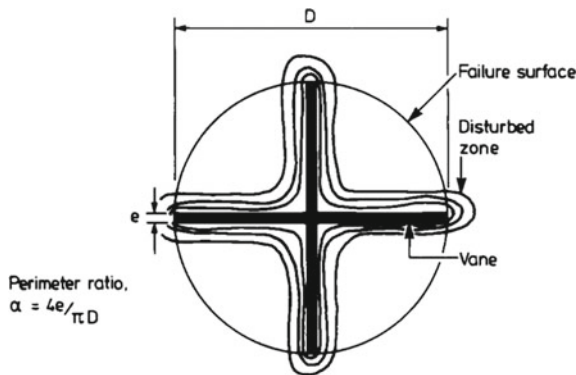
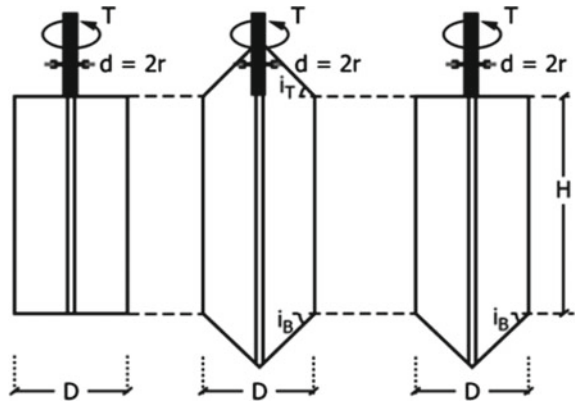


Fig. 1 The disturbance caused by the intrusion of the vane into the clay [3]

**Fig. 2** The geometry of field vane [1]



Variation in geometry vane size and shape can change the rate of soil shearing at constant rotation rate, which has resulted in analysis methods being generalized to consider shear rate in terms of peripheral vane velocity [2]. These methods account for variation in the shear surface (Fig. 2).

Yusoff et al. [18] carried out an experimental program on three vanes, 20 mm in diameter and height 20, 40, and 80 mm. The blades were rotated at a range of peripheral velocities from 0.5 to 400 mm/s to produce correlations of undrained shear strength and applied rate of shear. The outcomes of the investigation highlight that the peak shear resistance recorded increases with increasing peripheral velocity. The magnitude of vane displacement required to achieve full mobilization of soil shear strength was dependent on the applied rate of shear.

Mesri and Huvaj [9] stated that progressive failure affects all laboratory and in situ undrained shear tests. Mainly, undrained shear strength mobilized in a full-scale undrained failure in the field is, in general, not equal to the undrained shear strength measured by laboratory or in situ tests.

Thakur et al. [16] found that strain-softening can happen due to structural geometric instability and material instability. Most of the time, in common geotechnical engineering practice, the structural geometric weakness is ignored. However, softening material can be taken into account, such as fissuring and cracking. Referring to the underlying assumptions on field vane shear test assumes conservatively a fully mobilized cylindrical shear failure around the vane, indicating no progressive failure.

Griffiths and LANE [4] performed two-dimensional and quasi-three-dimensional finite element analysis of VST, considering the only tangential movement of material along with the blades of the vane. The conventional procedure for the mobilization of shear stresses are acceptable for isotropic, non-softening materials, with the peak shear stress distribution on the vane ends adequately modeled using a rectangular assumption. Their study determined that the conventional formula represents the best estimate for the cohesive strength of isotropic and non-softening soils.

Gylland et al. [6] investigated using in situ samples and numerical simulations to detect geometrical failure mode around the shear vane in soft sensitive clay. The global failure geometry is not a full cylinder, but rather a rounded square at the peak global torque. Finite element simulations strengthen these findings. Therefore, the correct assumption regarding the geometrical shape of the failure surface around the vane is essential for interpreting a correct shear strength value.

Gupta et al. [5] performed a numerical model to comprehend the undrained shear strength response of a saturated cohesive soil subjected to the vane shear test. The soil is modeled using the Mohr–Coulomb failure criteria and the response of soil until failure is studied. The result gives a higher value of the cohesive strength of clay from the measured rotation moment in a laboratory test. The respect of the stress distribution pattern in the numerical model shows that the expectations have a significant effect on the cohesive strength of soil as calculated from the maximum rotation moment.

Recently, Rismyhr [13] conducted numerical simulations to examine to which extent progressive failure (softening), anisotropy, and strain rate affect the measured strength from the shear vane test. The material models used were Mohr–Coulomb, Geo future Soft Clay (a user-defined material model developed by NTNU), and the total stress-based NGI ADP model using PLAXIS 2D and PLAXIS 3D.

### 3 Materials and Methodology

Main Characteristics of the vane apparatus and basic testing procedures design criteria for the device were taken from ASTM D2573–15 (Standard Test Method for Field Vane Shear Test in Cohesive Soil). Here are the common essential technical specifications.

The most commonly used vanes are with rectangular blades measuring 55 mm × 110 mm and the other with rectangular blades measuring 65 mm × 130 mm. Both vanes consist of four blades set at right angles. The larger and smaller vanes are capable of measuring undrained shear strength up to 50 kPa and 100 kPa, respectively [1].

Conventionally, it is interpreted that the applied torque is resisted by the shear stress mobilized along the failure surface. Since the test is carried out comparatively fast, undrained conditions can be assumed, and hence, the shear stress at failure is the same as the undrained shear strength,  $S_u$ , based on the schematic diagram shown in Fig. 3.

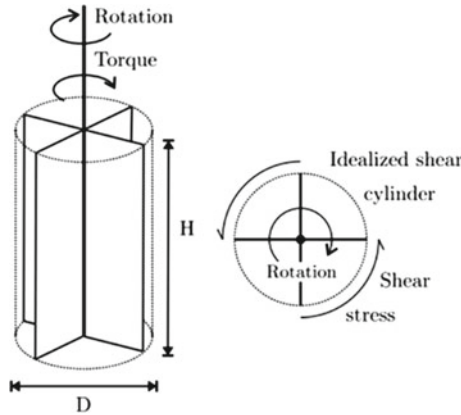


Fig. 3 Illustration of the shear vane (Gylland [6])

### 4 Finite Element Analysis in PLAXIS

The main features of the vane apparatus and the geometry used in the numerical simulations are based on the standard vane from the standard test method for field vane shear test in cohesive soil (ASTM D2573–15). The standard vane dimension used in this study is the height and diameter of 110 mm and 55 mm, respectively (Table 1).

The thicknesses of blades are also based on the standard to analyze the effect of blade thickness from 0.8 mm up to 3 mm. Soil contour has been defined based on the sensitivity analysis to ensure the boundary surfaces would not affect the results from the numerical simulations. The geometry of the problem is as shown in Fig. 4.

The input parameters of each material parameter were derived from the literature work [14]. The values of each material parameter were based on typical values for soft clay and stiff clay. The Mohr–Coulomb and Hardening soil model material parameters are summarized in Tables 2 and 3, respectively, and material parameters of the plate blades are shown in Table 4.

Undrained (A) is used for calculation of undrained or short-term material behavior in which stiffness and strength are defined in terms of effective properties. A significant bulk stiffness for water is automatically applied to make the soil as a whole incompressible, and (excess) pore pressures are calculated, even above the phreatic surface.

The default boundary conditions were used as in PLAXIS 3D settings as shown in Fig. 5. The horizontal bottom boundary was fully fixed. The vertical boundaries were set in horizontal movement and free in a vertical movement. The top horizontal boundary was free in all directions.

Conditions for cylinder boundaries are also set on; in particular, displacements along all directions are free. Furthermore, conditions about displacements on blades are needed: while vertical displacements on tips are fixed, x and y displacements are

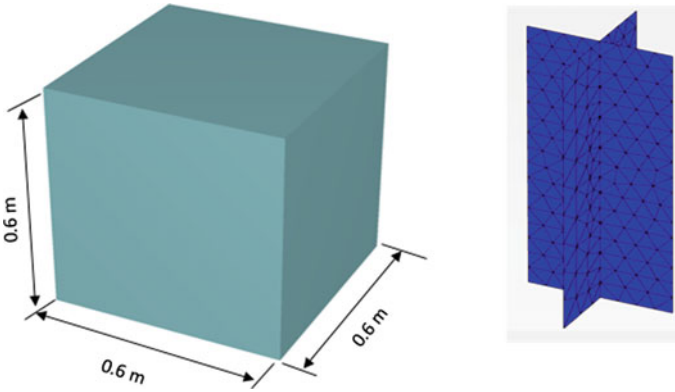


**Fig. 4** Soil and Vane model in Plaxis

**Table 1** Proposed formulae for estimating lateral soil resistance

Parameters	Standard (ASTM D2573–15)
Vane diameter (D)	35–100 mm
Vane shaft diameter (d)	12.5–16.5 mm
Vane height (H)	$1D \leq H \leq 2.5D$
Blade thickness (e)	$e < 3 \text{ mm}$
Taper angle (i)	Usually 0 degrees (rectangular) or 45 degrees (tapered)
Vane area ratio	Less than 12%

**Table 2** Mohr–Coulomb material parameters used in finite element models

Parameters	Symbol	Soil type	
		Soft clay	Stiff clay
Type of material behavior		Undrained (A)	Undrained (A)
Soil unit weight ( $\text{kN/m}^3$ )	$\gamma_{unsat}$	16	17
	$\gamma_{sat}$	18	19
Young’s modulus	$E_{ref}$	3000	4000
Poisson’s ratio	$\nu$	0.3	0.3
Cohesion	$C_{ref}$	1	10
Friction angle	$\phi$	15°	28°
Dilatancy angle	$\psi$	0°	0°

free; displacements are also fixed on the blades’ crossing vertical line using the line displacement at the tips of the vane blade as shown in Fig. 6 below.

PLAXIS 3D provides various geometric entities that are the basic components of the physical model. Structures and loads can be assigned to the geometric objects.

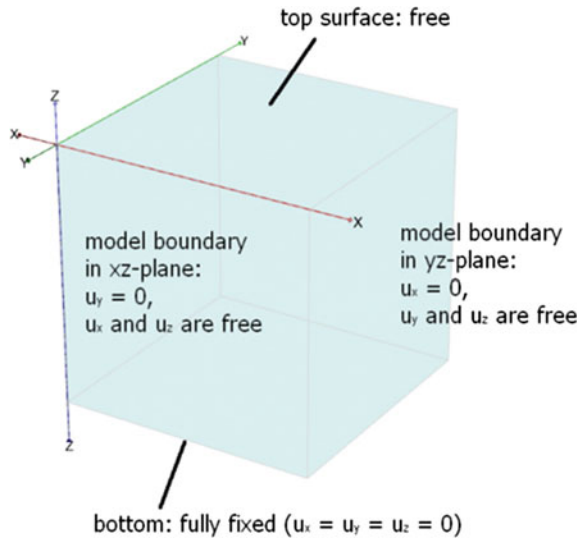
**Table 3** Hardening soil model material parameters used in finite element models

Parameters	Symbol	Soil type	
		Soft clay	Stiff Clay
Type of material behavior		Undrained (A)	Undrained (A)
Soil unit weight (kN/m <sup>3</sup> )	$\gamma_{unsat}$	16	17
	$\gamma_{sat}$	18	19
Stiffness	$E^{ref}_{50}$	3000	6000
	$E^{ref}_{oed}$	3700	6000
	$E^{ref}_{ur}$	9000	18,000
	$Power(m)$	1	0.8
	$\nu_{ur}$	0.2	0.2
Strength	$C'_{ref}$	1	10
	$\phi'$	15°	28°
	$\Psi'$	0°	0°

**Table 4** Plate blade material parameters

Parameters	Standard (ASTM D2573–15)
Vane shaft diameter (d)	3 mm
Unit weight ( $\gamma$ )	77 kN/m <sup>3</sup>
E1	$2.1 \times 10^8$
E2	$2.1 \times 10^8$
$\nu_{12}$	0.495

**Fig. 5** Boundary conditions in PLAXIS 3D [12]



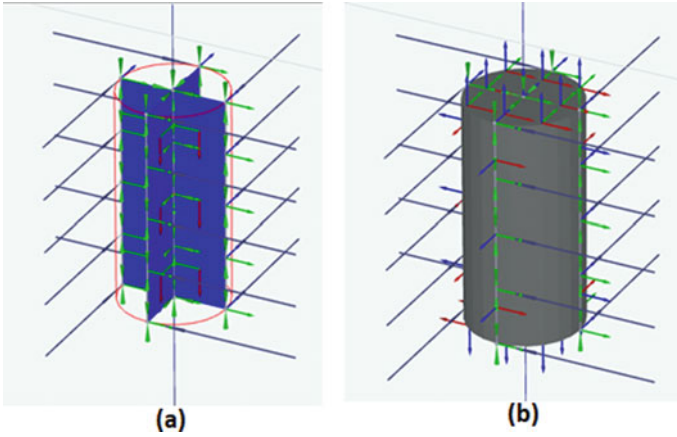


**Fig. 6** a Creating line displacements at the tip of each blade and the center of the vane; b Conditions for cylinder boundaries along all directions are free

The vane blades in PLAXIS 3D can be modeled using plate elements. The material properties of plates are contained in material data sets. The vane blade was modeled in the PLAXIS 3D structure option as a plate with its properties in the material and methods section.

Torque was simulated by applying line loads at the end of each blade. Initially, there were some problems regarding the rotation of the vane. To ensure rotation of the vane, line displacements at the tip and center blade of the vane were created. Each tip was fixed in the x and y direction and free in the z-direction. The center of the vane was fixed in the x, y, and z-direction as shown in Fig. 7.

**Fig. 7** Line load at the tip of each blade to simulate the torque at failure

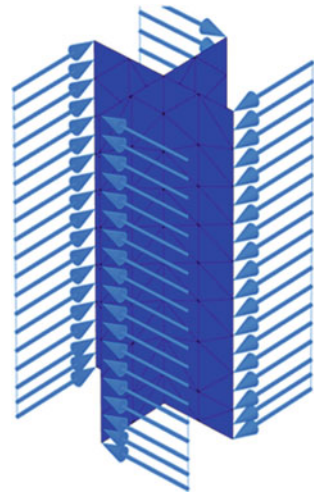
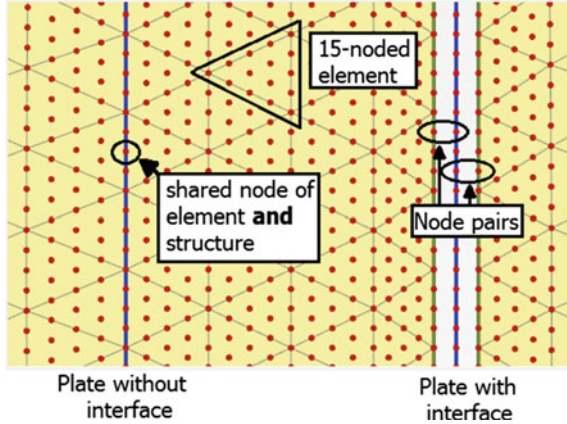




**Fig. 8** PLAXIS interface soil-plate layout [12]



To simulate the interaction between the soil and a structure, in this case, the plate, PLAXIS uses interface elements. Without any interface, the structure and the soil are tied together with no relative displacement (slipping/gapping) possible between the structure and the soil. By using an interface, node pairs are created at the interface of structure and soil, one belonging to the soil and the other to the plate. The interaction between the nodes consists of two elastic-perfectly plastic springs, as shown in Fig. 8, the first one models the gap displacement, and the second the slipping displacement.

### 4.1 Numerical Simulation

The finite element models were modeled having the same dimension as the theoretical calculation used. Both Mohr–Coulomb and Hardening soil material models were considered for both stiff clay and soft clay soils.

As shown in Fig. 9 exported from the PLAXIS 3D tables, the  $\sum M_{stage}$ , which percentage of the assigned basic load applied on the vane blade tip is 0.119, declares that 11.9% of the primary line load, 25 kN/m, is applied on the vane blade, and it reached its failure using the Mohr–Coulomb material model for the case of stiff clay soil.

The torque at failure for Stiff clay was obtained from PLAXIS simulation via Hardening soil model and Mohr–Coulomb 33.275 Nm and 35.997 Nm, respectively. The hardening soil model fits well with the result from the theoretical calculation 33.275 Nm and 33.53 Nm, respectively. The Percentage of difference for theoretical calculation and numerical simulation using the hardening soil model and Mohr–Coulomb is 0.76% and 8.1%, respectively. Whereas for soft clay, it opts out to be 0.76% and 9.46%, respectively.

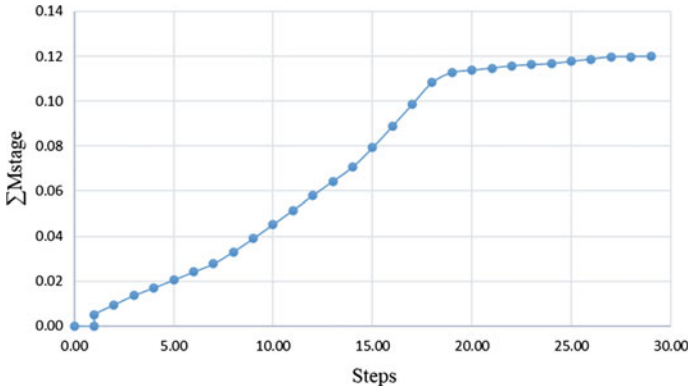


Fig. 9 Ultimate line loading in vane tips

### 4.2 Effect of Blade Thickness

Four field vane were simulated, having different perimeter ratios ranging from 1.4 to 6.01%. The vanes were rectangular, four-bladed vanes with heights of 110 mm and diameters of 55 mm, given that height to diameter ratios of two. The only difference then was the blade thickness (0.8, 1.4, 2.0, and 2.6 mm). The blade thickness was different to offer different values of  $\alpha$ . The diameter of the vanes and height was held constant. Table 3.1 presents the vane dimensions (Fig. 10).

Field Vane test undrained shear strengths are directly interrelated to the thickness of vane blades used within perimeter ratios ranging from 1.4 to 6.01%. The results from four simulations showing that the measured undrained shear strengths are inversely proportional to the perimeter ratio of the vane well agreed with [3,

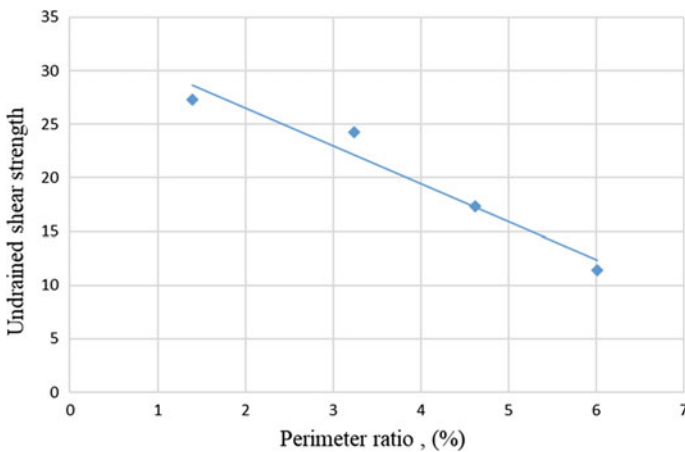
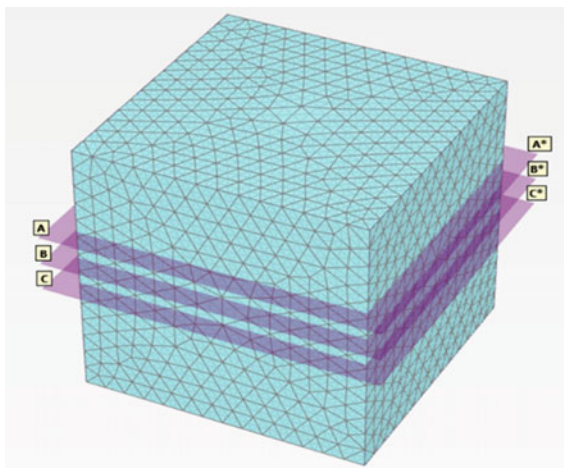


Fig. 10 Result of undrained shear strength versus perimeter ratio

**Fig. 11** The sections of the model



15] findings. Undrained strength values approximately 27.28 kN and ( $\alpha = 1.4\%$ ) when compared with Undrained strength 23.4 kN and ( $\alpha = 3.24\%$ ), the percentage of difference is 12.26%. As a result, with the same type of soil but different blade thickness, the undrained shear strength can vary significantly (Fig. 11).

### 4.3 Further Analysis

The evolution of plastic points increasing rotation close to the peak resistance is presented in Fig. 12. Red plastic points are material regions at the MC line. The evolution of these indicated that elements of progressive failure are present before the peak global resistance is reached.

## 5 Conclusions

From the Vane shear analysis in PLAXIS, the following conclusions can be drawn.

1. The results for both soft and stiff clay soils using the Mohr–Coulomb gave too large the torque at failure and the big difference between simulated and hand calculation with the percentage of difference for stiff clay soil 8.1% and soft clay soil 9.46%, respectively.
2. The hardening soil model fits well with the result compared to both measured stiff and soft soil between hand calculation and numerical simulation with a percentage of 0.76% for both cases.

Top section A-A\* (z=0.2 m) displacement and plastic points

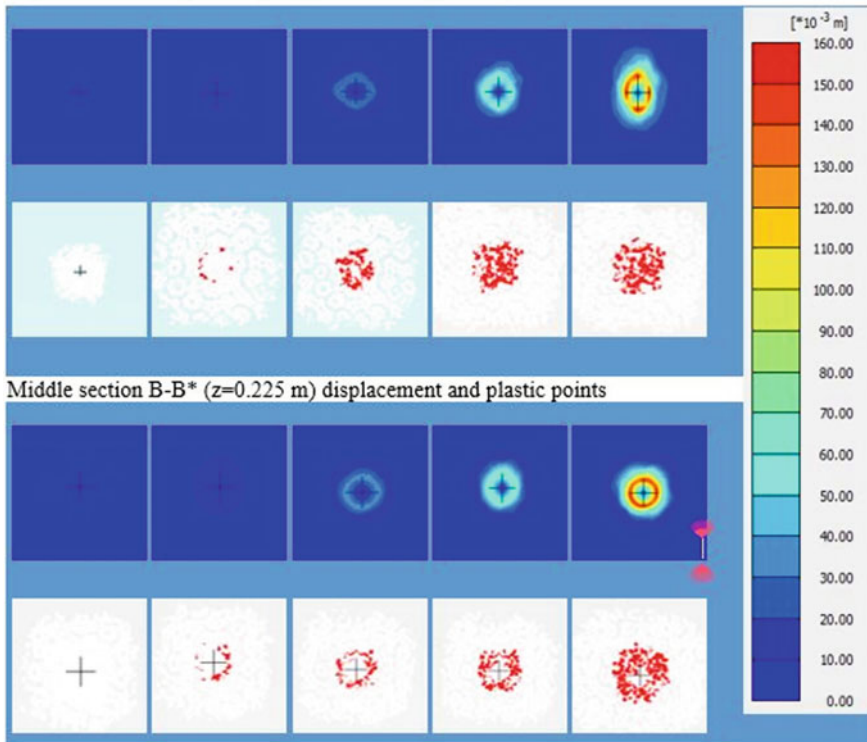


**Fig. 12** Results of displacements (u) and evolution of plastic points around the vane during rotation; plastic points refer, respectively, to the top and middle of the vane

3. The result of the four simulations shows for the same type of soil with different blade thickness; the undrained shear strength can vary significantly approximately 27.28 kN for  $\alpha = 1.4\%$  and compared with undrained strength 23.4 kN for  $\alpha = 3.24\%$  gives the percentage of difference 12.26%.
4. The measured undrained shear strengths are inversely proportional to the perimeter ratio of the vane well agreed with other previous findings.
5. The failure geometry around the blade is recognized in the plastic point's picture, more emphasized at the top than in the middle of the device.

## References

1. In Standard Test Method for Field Vane Shear Test in Saturated Fine-Grained Soils, pp. 1–8. <https://doi.org/10.1520/D2573>
2. Biscontin, G., Pestana, J.: Influence of peripheral velocity on measurements of undrained shear strength for an artificial soil. In: Geotechnical Engineering Report No UCB/GT/99-19 (2000). <http://www.ce.berkeley.edu/~pestana/reports/UCBGT99-19 Effect of Peripheral.pdf>
3. Cerato, A.B., Lutenegeger, A. J.: Disturbance effects of field vane tests in a varved clay. In: Proceedings of the 2nd International Conference on Geotechnical and Geophysical Site Characterization, October, pp. 861–867 (2004). <http://faculty-staff.ou.edu/C/Amy.B.Cerato-1/cerato.pdf>
4. Griffiths, D., Lane, P.A.: Finite element analysis of the shear vane test. *37*(6), 1105–1116 (1990)
5. Gupta, T., Chakraborty, T., Abdel-Rahman, K., Achmus, M.: Large deformation finite element analysis of Vane Shear tests. *Geotech. Geol. Eng.* **34**(5), 1669–1676 (2016). <https://doi.org/10.1007/s10706-016-0048-0>
6. Gylland, A.S.: Microstructural Observations of Shear Zones in Sensitive Clay. Norwegian University of Science and Technology (2012)
7. Gylland, A.S., Jostad, H.P., Nordal, S.: Failure geometry around a shear vane in sensitive clay. In: NGM 2012 Proceedings, pp. 103–110 (2012)
8. Jonsson, M., Sellin, C.: Correction of shear strength in cohesive soil (2012)
9. Mesri, G., Huvaj, N.: Shear strength mobilized in undrained failure of soft clay and silt deposits. In: Advances in Measurement and Modeling of Soil Behavior (2007)
10. Morin, P.J.J.: Vane shear strength testing in soils, field, and laboratory studies. *ASTM* **27**(1), 165–165 (1990). <https://doi.org/10.1139/t90-018>
11. Peuchen, J., Mayne, P.: Rate effects in vane shear testing. In: Proceedings of the 6th International Offshore Site Investigation and Geotechnics Conference: Confronting New Challenges and Sharing Knowledge, OSIG 2007, pp. 187–194 (2007)
12. PLAXIS.: User's manual (2013)
13. Rismyhr, K.: Effect of Anisotropy, Strain Rate and Progressive Failure in Numerical Simulations of the Shear Vane Test (Issue June) (2017)
14. Susila, E., Apoji, D.: Settlement of a full scale trial Embankment on Peat in Kalimantan: field measurements and finite element simulations. *Jurnal Teoretis Dan Terapan Bidang Rekayasa Sipil* **19**(0853–2982), 249–269 (2012)
15. Terzaghi, K., Peck, R., Mesri, G.: (1996) *Soil Mechanics in Engineering Practice*, 3rd edn. Wiley, New York
16. Thakur, V., Nordal, S., Grimstad, G.: Phenomenological issues related to strain localization in sensitive clays. *Geotech. Geol. Eng.* **24**(6), 1729–1747 (2006). <https://doi.org/10.1007/s10706-005-5818-z>
17. Wilson, L.J., Kouretzis, G.P., Pineda, J.A., Kelly, R.B.: On the determination of the undrained shear strength from vane shear testing in soft clays. In: Proceedings of the 5th International Conference on Geotechnical and Geophysical Site Characterisation, ISC 2016, pp. 455–460 (2016)
18. Yusoff, N., Black, J.A., Hyde, A.F.: Rate effects and vane shear strength of sandy clay (2018)